

Measuring the cosmological parameters with the $E_{p,i} - E_{iso}$ correlation of Gamma-Ray Bursts

Lorenzo Amati^{1*}, Cristiano Guidorzi², Filippo Frontera^{1,3}, Massimo Della Valle^{4,5,6},
Fabio Finelli^{1,7,8}, Raffaella Landi¹ and Enrico Montanari^{3,9}

¹INAF - IASF Bologna, via P. Gobetti 101, I-40129 Bologna (Italy)

²INAF - Osservatorio Astronomico di Brera, via Bianchi, 46, I-23807 Merate (LC), Italy

³Dipartimento di Fisica, Università di Ferrara, via Saragat 1, I-44100 Ferrara, Italy

⁴INAF - Osservatorio Astronomico di Capodimonte, Salita Moiarriello, 16 I-80131 Napoli (Italy)

⁵European Southern Observatory - Karl Schwarzschild Strasse 2, Garching bei Munchen (Germany)

⁶International Centre for Relativistic Astrophysics Network-Piazzale della Repubblica 2, Pescara (Italy)

⁷INAF - Osservatorio Astronomico di Bologna, via Ranzani 1, I-40127 Bologna (Italy)

⁸INFN, Sezione di Bologna, Via Irnerio 46, I-40126 Bologna (Italy)

⁹I.I.S. "I. Calvi", via Digione, 20, I-41034 Finale Emilia (MO), Italy

Submitted 2008 May 3.

ABSTRACT

We have used the $E_{p,i} - E_{iso}$ correlation of GRBs to measure the cosmological parameter Ω_M . By adopting a maximum likelihood approach which allows us to correctly quantify the extrinsic (i.e. non-Poissonian) scatter of the correlation, we constrain (for a flat universe) Ω_M to 0.04–0.40 (68% confidence level), with a best fit value of $\Omega_M \sim 0.15$, and exclude $\Omega_M = 1$ at $> 99.9\%$ confidence level. If we release the assumption of a flat universe, we still find evidence for a low value of Ω_M (0.04–0.50 at 68% confidence level) and a weak dependence of the dispersion of the $E_{p,i} - E_{iso}$ correlation on Ω_Λ (with an upper limit of $\Omega_\Lambda \sim 1.15$ at 90% confidence level). Our approach makes no assumptions on the $E_{p,i} - E_{iso}$ correlation and it does not use other calibrators to set the “zero” point of the relation, therefore our treatment of the data is not affected by circularity and the results are independent of those derived via type Ia SNe (or other cosmological probes). Unlike other multi-parameters correlations, our analysis grounds on only two parameters, then including a larger number (a factor ~ 3) of GRBs and being less affected by systematics. Simulations based on realistic extrapolations of ongoing (and future) GRB experiments (e.g., *Swift*, *Konus-Wind*, *GLAST*) show that: i) the uncertainties on cosmological parameters can be significantly decreased; ii) future data will allow us to get clues on the “dark energy” evolution.

Key words: gamma-rays: observations – gamma-rays: bursts – cosmology: cosmological parameters.

1 INTRODUCTION

Gamma-ray Bursts (GRBs) are the brightest cosmological sources in the universe, with isotropic luminosities up to 10^{54} erg cm^{−2} s^{−1} and a redshift distribution extending at least up to $z \sim 6.3$ (e.g., Tagliaferri et al. 2005). Thus, these sources may be interesting for cosmological studies, if one can use them to provide measurements of the cosmological parameters independently of other methods, like the CMB (e.g., De Bernardis et al. 2000; Spergel et al. 2003; Dunkley et al. 2008; Komatsu et al. 2008), type Ia SN

(e.g., Perlmutter et al. 1998; Perlmutter et al. 1999; Riess et al. 1998; Riess et al. 2004; Astier et al. 2006), Baryon Acoustic Oscillations (BAO) (e.g., Eisenstein et al. 2005; Tegmark et al. 2006; Percival et al. 2007), galaxy clusters (e.g., Rosati, Borgani & Norman 2002; Voit 2005). However, GRBs are not standard candles, given that their luminosities span several orders of magnitude under the assumption of both isotropic and collimated emission (e.g., Ghirlanda et al. 2006). In the recent years, several attempts to “standardize” GRB have been made, mainly on the basis of correlations involving: a) a GRB intensity indicator, like the isotropic-equivalent radiated energy (E_{iso}) or the isotropic-equivalent peak luminosity ($L_{p,iso}$); b) the photon energy

* E-mail: amati@iasfbo.inaf.it

at which the time averaged νF_ν spectrum peaks ("peak energy", $E_{p,i}$); c) other observables, like the break time of the afterglow light curve, t_b , or the "high signal time scale" $T_{0.45}$ (Ghirlanda, Ghisellini & Lazzati 2004; Firmani et al. 2006). Finally, Schaefer (2007) used different correlations (spectrum–energy, time lag – luminosity, peak luminosity – variability) to construct a GRB Hubble diagram and constrain the cosmological parameters.

These analyses have provided useful constraints on Ω_M and Ω_Λ consistent with those derived from type Ia SNe, see, e.g., Ghirlanda et al. (2006) for a review. However, the use of these correlations for cosmology is controversial. For example, because of the lack of low redshift GRBs they cannot be directly calibrated. On the other hand the calibration of a spectrum–energy correlation using SNe-Ia as calibrators (Kodama et al. 2008; Liang et al. 2008) is an interesting attempt to use GRBs as cosmological probes, but it may look suspicious that this method gives very similar results to those obtained via SNe. Thus, particular care and sophisticated statistical methodologies have to be adopted in order to avoid circularity problems when constructing a GRB Hubble diagram. In addition, recent analyses based on updated samples of GRBs showed that the dispersion of three–parameter correlations could be significantly larger than thought before (Campana et al. 2007; Ghirlanda et al. 2007; Rossi et al. 2008).

In this article we investigate the possibility of constraining the cosmological parameters from the $E_{p,i} - E_{iso}$ correlation. This correlation was initially discovered on a small sample of *BeppoSAX* GRBs with known redshift (Amati et al. 2002) and confirmed afterwards by *Swift* observations (Amati 2006). Although it was the first "spectrum–energy" correlation discovered for GRBs (and the most firmly established one, to date) it was never used for cosmology purposes, because of its significant "extrinsic" scatter (i.e., a scatter in excess to the "intrinsic" Poissonian fluctuations of the data). However, the conspicuous increasing of GRB discoveries combined with the fact that $E_{p,i} - E_{iso}$ correlation needs only two parameters that are directly inferred from observations (this fact minimizes the effects of systematics and increases the number of GRBs that can be used, by a factor ~ 3) makes the use of this correlation an interesting tool for cosmology.

Our study was motivated by our finding that, in the assumption of a flat universe, the χ^2 obtained by fitting the $E_{p,i} - E_{iso}$ correlation with a power-law varies with the value of Ω_M assumed to compute E_{iso} , has its minimum value for $\Omega_M \sim 0.25$, very close the value obtained with SNe-Ia approach. In this paper we show indeed that a small fraction of the extrinsic scatter is due to the choice of cosmological parameters, thus allowing us to constrain Ω_M and, to a smaller extent, Ω_Λ .

2 THE UPDATED $E_{p,i} - E_{iso}$ SAMPLE

Previous analyses of the $E_{p,i} - E_{iso}$ plane of GRBs shows that different classes of GRBs exhibit different behaviours: while normal long GRBs and X-Ray Flashes (XRF, i.e. particularly soft bursts) follow the $E_{p,i} - E_{iso}$ correlation, short GRBs and the peculiar very close and sub-energetic GRB 980425 do not (Amati et al. 2007). Therefore, in our

analysis we considered only long GRB/XRF. The sample of long GRB/XRF used in this paper (updated to April, 11 2008) is reported in Table 1 and includes 70 GRBs. We report, for each GRB, the redshift, the fluence and the cosmological rest-frame spectral peak energy, $E_{p,i} = E_{p,obs} \times (1+z)$. The redshift distribution covers a broad range of z , from 0.033 to 6.3, thus extending far beyond that of Type Ia SNe ($z < \sim 1.7$). For *Swift* GRBs, the $E_{p,i}$ value derived from BAT spectral analysis alone were conservatively taken from the results reported by the BAT team (Sakamoto et al. 2008a,b). Other BAT $E_{p,i}$ values reported in the literature were not considered, because either they were not confirmed by Sakamoto et al. (2008a,b) refined analysis (e.g., Cabrera et al. 2007) or they are based on speculative methods (Butler et al. 2007).

In Table 1 we also report the values of E_{iso} computed from published spectral parameters and fluences by following the standard method described, e.g., by Amati (2006) and assuming $H_0 = 70 \text{ km s}^{-1} \text{ Mpc}^{-1}$, $\Omega_M = 0.3$ and $\Omega_\Lambda = 0.7$ (references are reported in Table 1). An analysis of Figure 1 (left panel) shows that, for this "standard" cosmology, all GRBs in our sample follow the $E_{p,i} - E_{iso}$ correlation; in particular, *Swift* GRBs are well consistent with the $E_{p,i} - E_{iso}$ correlation based on GRBs discovered by other instruments characterised by different trigger thresholds and sensitivities (as a function of energy). This fact points out that the $E_{p,i} - E_{iso}$ correlation is not affected by significant selection effects (see also Ghirlanda et al. 2008).

If we fit the data of Figure 1 with a simple power-law, we find an index $m = 0.57 \pm 0.01$ and a normalization $K = 94 \pm 2$, consistent with results of previous analyses (e.g., Amati 2006). However, despite the very high significance of the correlation (Spearman's $\rho = 0.872$ for 70 events), the fit with a power-law provides an highly unacceptable χ^2_ν value (408/68). This is clear evidence of the existence of a significant extrinsic scatter, which is superimposed to the Poissonian one and implies the existence of "hidden" parameters, connected with GRB phenomenology, which contribute to define the location of a GRB in the $E_{p,i} - E_{iso}$ plane. It should be noted that systematics affecting both $E_{p,i}$ and E_{iso} may contribute to the extrinsic scatter, even if there is evidence that they are not a dominant component (Landi et al. 2006).

3 COSMOLOGICAL PARAMETERS DERIVED FROM THE $E_{p,i} - E_{iso}$ CORRELATION

The main goal of this paper is to investigate if the extrinsic dispersion of the $E_{p,i} - E_{iso}$ correlation is sensitive at varying the values of the cosmological parameters Ω_M and Ω_Λ . We emphasize that this method does not suffer from circularity, since we do not assume an $E_{p,i} - E_{iso}$ relation based on a particular choice of the cosmological parameters or calibrate it by using other cosmological probes.

As a first step, under the assumption of a flat universe, we studied the trend of the χ^2 values obtained by fitting the $E_{p,i} - E_{iso}$ correlation with a simple power-law, for different choices of Ω_M . Here and in the following, we assumed $H_0 = 70 \text{ km s}^{-1} \text{ Mpc}^{-1}$. Figure 2 (left) shows that the extrinsic scatter of the correlation indeed decreases with cosmology, and minimizes for $\Omega_M \sim 0.25$. This result is

Table 1. Values of redshift, "bolometric" fluence and cosmological rest-frame spectral peak energy, $E_{p,i}=E_{p,obs}\times(1+z)$, of long GRBs and XRFs with firm estimates of both z and $E_{p,obs}$ (70 events) as of April, 11 2008. These are the values that we used to estimate cosmological parameters. The table includes also the values of E_{iso} computed by assuming $H_0 = 70 \text{ km s}^{-1} \text{ Mpc}^{-1}$, $\Omega_M = 0.3$ and $\Omega_\Lambda = 0.7$. The uncertainties are at 1σ significance. The "Instruments" column reports the name of the experiment(s), or of the satellite(s), that provided the estimates of spectral parameters and fluence (GRO = CGRO/BATSE, SAX = *Beppo*SAX, HET = HETE-2, KW = Konus-Wind, SWI = *Swift*). The last column reports the references for the spectral parameters used to derive the fluence and $E_{p,i}$. Redshift values were taken from the GRB table by J. Greiner and references therein (<http://www.mpe.mpg.de/~jcg/grbgen.html>).

GRB	z	Fluence ^(a) ($10^{-5} \text{ erg cm}^{-2}$)	$E_{p,i}$ (keV)	E_{iso} ^(b) (10^{52} erg)	Instruments	Refs. for ^(c) spectrum
970228	0.695	1.3±0.1	195±64	1.60±0.12	SAX	(1)
970508	0.835	0.34±0.07	145±43	0.61±0.13	SAX	(1)
970828	0.958	12.3±1.4	586±117	29±3	GRO	(1)
971214	3.42	0.87±0.11	685±133	21±3	SAX	(1)
980326	1.0	0.18±0.04	71±36	0.48±0.09	SAX	(1)
980613	1.096	0.19±0.03	194±89	0.59±0.09	SAX	(1)
980703	0.966	2.9±0.3	503±64	7.2±0.7	GRO	(1)
990123	1.60	35.8±5.8	1724±466	229±37	SAX/GRO/KW	(1)
990506	1.30	21.7±2.2	677±156	94±9	GRO/KW	(1)
990510	1.619	2.6±0.4	423±42	17±3	SAX	(1)
990705	0.842	9.8±1.4	459±139	18±3	SAX/KW	(1)
990712	0.434	1.4±0.3	93±15	0.67±0.13	SAX	(1)
991208	0.706	17.2±1.4	313±31	22.3±1.8	KW	(1)
991216	1.02	24.8±2.5	648±134	67±7	GRO/KW	(1)
000131	4.50	4.7±0.8	987± 416	172±30	GRO/KW	(1)
000210	0.846	8.0±0.9	753±26	14.9±1.6	KW	(1)
000418	1.12	2.8±0.5	284±21	9.1±1.7	KW	(1)
000911	1.06	23.0±4.7	1856±371	67±14	KW	(1)
000926	2.07	2.6±0.6	310±20	27.1±5.9	KW	(1)
010222	1.48	14.6±1.5	766±30	81±9	KW	(1)
010921	0.450	1.8±0.2	129±26	0.95±0.10	HET	(1)
011121	0.36	24.3±6.7	1060±265	7.8±2.1	SAX/KW	(2)
011211	2.14	0.50±0.06	186±24	5.4±0.6	SAX	(1)
020124	3.20	1.2±0.1	448±148	27±3	HET/KW	(1)
020405	0.69	8.4±0.7	354±10	10±0.9	SAX/KW	(2)
020813	1.25	16.3±4.1	590±151	66±16	HET/KW	(1)
020819B	0.410	1.6±0.4	70±21	0.68±0.17	HET	(1)
020903	0.250	0.016±0.004	3.37±1.79	0.0024±0.0006	HET	(1)
021004	2.30	0.27±0.04	266±117	3.3±0.4	HET	(1)
021211	1.01	0.42±0.05	127±52	1.12±0.13	HET/KW	(1)
030226	1.98	1.3±0.1	289±66	12.1±1.3	HET	(1)
030323	3.37	0.12±0.04	270±113	2.8±0.9	HET	(3)
030328	1.52	6.4±0.6	328±55	47±3	HET/KW	(1)
030329	0.17	21.5±3.8	100±23	1.5±0.3	HET/KW	(1)
030429	2.65	0.14±0.02	128±26	2.16±0.26	HET	(1)
030528	0.78	1.4±0.2	57±9.0	2.5±0.3	HET	(3)
040912	1.563	0.21±0.06	44±33	1.3±0.3	HET	(4)
040924	0.859	0.49±0.04	102±35	0.95±0.09	HET/KW	(1)
041006	0.716	2.3±0.6	98±20	3.0±0.9	HET	(1)
050318	1.44	0.42±0.03	115±25	2.20±0.16	SWI	(1)
050401	2.90	1.9±0.4	467±110	35±7	KW	(1)
050416A	0.650	0.087±0.009	25.1±4.2	0.10±0.01	SWI	(1)
050525A	0.606	2.6±0.5	127±10	2.50±0.43	SWI	(1)
050603	2.821	3.5±0.2	1333±107	60±4	KW	(1)
050820	2.612	6.4±0.5	1325±277	97.4±7.8	KW	(5)
050904	6.29	2.0±0.2	3178±1094	124±13	SWI/KW	(6)
050922C	2.198	0.47±0.16	415±111	5.3±1.7	HET	(1)
051022	0.80	32.6±3.1	754±258	54±5	HET/KW	(1)
051109A	2.346	0.51±0.05	539±200	6.5±0.7	KW	(1)
060115	3.53	0.25±0.04	285±34	6.3±0.9	SWI	(7)
060124	2.296	3.4±0.5	784±285	41± 6	KW	(8)
060206	4.048	0.14±0.03	394±46	4.3±0.9	SWI	(7)
060218	0.0331	2.2±0.1	4.9±0.3	0.0053±0.0003	SWI	(9)
060418	1.489	2.3±0.5	572±143	13±3	KW	(10)

GRB	z	Fluence ^(a) (10^{-5} erg cm $^{-2}$)	$E_{p,i}$ (keV)	E_{iso} ^(b) (10^{52} erg)	Instruments	Refs. for ^(c) spectrum
060526	3.21	0.12 \pm 0.06	105 \pm 21	2.6 \pm 0.3	SWI	(11)
060614	0.125	5.9 \pm 2.4	55 \pm 45	0.21 \pm 0.09	KW	(12)
060707	3.425	0.23 \pm 0.04	279 \pm 28	5.4 \pm 1.0	SWI	(7)
060814	0.84	3.8 \pm 0.4	473 \pm 155	7.0 \pm 0.7	KW	(13)
060908	2.43	0.73 \pm 0.07	514 \pm 102	9.8 \pm 0.9	SWI	(7)
060927	5.60	0.27 \pm 0.04	475 \pm 47	13.8 \pm 2.0	SWI	(7)
061007	1.261	21.1 \pm 2.1	890 \pm 124	86 \pm 9	KW/SUZ	(14)
061121	1.314	5.1 \pm 0.6	1289 \pm 153	22.5 \pm 2.6	KW/SUZ	(15)
061126	1.1588	8.7 \pm 1.0	1337 \pm 410	30 \pm 3	SWI/RHE	(16)
070125	1.547	13.3 \pm 1.3	934 \pm 148	80.2 \pm 8.0	KW	(17)
071010B	0.947	0.74 \pm 0.37	101 \pm 20	1.7 \pm 0.9	KW	(18)
071020	2.145	0.87 \pm 0.40	1013 \pm 160	9.5 \pm 4.3	KW	(19)
071117	1.331	0.89 \pm 0.21	647 \pm 226	4.1 \pm 0.9	KW	(20)
080319B	0.937	49.7 \pm 3.8	1261 \pm 65	114 \pm 9	KW	(21)
080319C	1.95	1.5 \pm 0.3	906 \pm 272	14.1 \pm 2.8	KW	(22)
080411	1.03	5.7 \pm 0.3	524 \pm 70	15.6 \pm 0.9	KW	(23)

Notes. (a) Bolometric fluence computed in the $[1/(1+z) - 10000/(1+z)]$ keV energy range.

(b) Computed by assuming $H_0 = 70$ km s $^{-1}$ Mpc $^{-1}$, $\Omega_M = 0.3$ and $\Omega_\Lambda = 0.7$.

(c) References for the spectral parameters and for the values and uncertainties of $E_{p,i}$ and E_{iso} : (1) Amati (2006) and references therein; (2) Ulanov et al. (2005) and refined analysis of *BeppoSAX* data; (3) Sakamoto et al. (2005); (4) Stratta et al. (2006); (5) Cenko et al. (2006); (6) Krimm et al. (2006); (7) Sakamoto et al. (2008a); (8) Golenetskii et al. (2006a); (9) Campana et al. (2006); (10) Golenetskii et al. (2006b); (11) Schaefer (2007) and references therein; (12) Amati et al. (2007) and references therein; (13) Golenetskii et al. (2006c); (14) Mundell et al. (2007) and references therein; (15) Ghirlanda et al. (2007) and references therein; (16) Perley et al. (2008); (17) Golenetskii et al. (2007a); (18) Golenetskii et al. (2007b); (19) Golenetskii et al. (2007c); (20) Golenetskii et al. (2007d); (21) Golenetskii et al. (2008a); (22) Golenetskii et al. (2008b); (23) Golenetskii et al. (2008c).

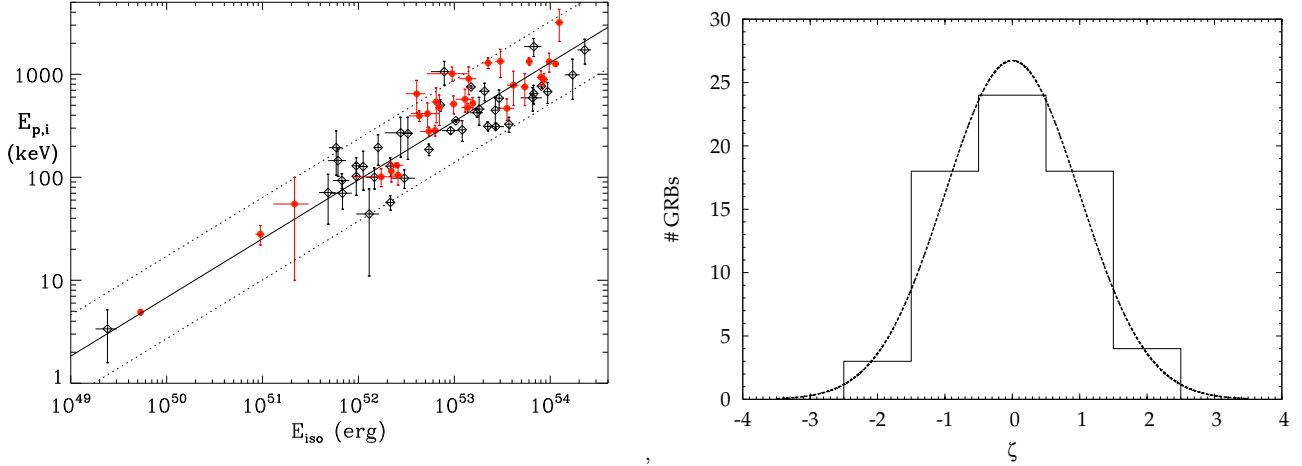


Figure 1. Left: location in the $E_{p,i} - E_{iso}$ plane of the 70 GRBs and XRFs with firm estimates of redshift and $E_{p,obs}$ included in our sample (E_{iso} computed following Amati (2006) and assuming a cosmology with $H_0 = 70$ km s $^{-1}$ Mpc $^{-1}$, $\Omega_M = 0.3$ and $\Omega_\Lambda = 0.7$). Red dots are *Swift* GRBs. Black dots are GRBs discovered by other satellites. The best-fit power-law is the continuous line ($\pm 2\sigma_{ext}$ region). Right: distribution of the normalised scatter (see, e.g., Rossi et al. 2008 for definition and method) of the $E_{p,i} - E_{iso}$ correlation for $H_0 = 70$ km s $^{-1}$ Mpc $^{-1}$, $\Omega_M = 0.3$ and $\Omega_\Lambda = 0.7$; the normalised Gaussian is superimposed to the data.

in qualitative agreement with the one obtained, e.g., with SNe (Perlmutter et al. 1998, 1999; Riess et al. 1998, 2004; Astier et al. 2006).

In order to better characterize the dependence of the $E_{p,i} - E_{iso}$ extrinsic scatter on cosmology, we have used the maximum likelihood method (hereafter MLM) as discussed by D’Agostini (2005) (see also Guidorzi et al. 2006, Amati 2006 and Rossi et al. 2008 for other applications of this methodology). This method assumes that, if the cor-

related data (x_i, y_i) can be described by a linear function $Y = mX + q$ with the addition of an extrinsic scatter σ_{ext} among the free parameters, the optimal values of the parameters (m , q , and σ_{ext}) can be obtained by minimizing the $-\log(\text{likelihood})$ function, in which the uncertainties on both (x_i, y_i) are taken into account. The general $\log(\text{likelihood})$ function is given by:

$$\log p(m, q, \sigma_x, \sigma_y | \{x_i, y_i, \sigma_{x,i}, \sigma_{y,i}\}) =$$

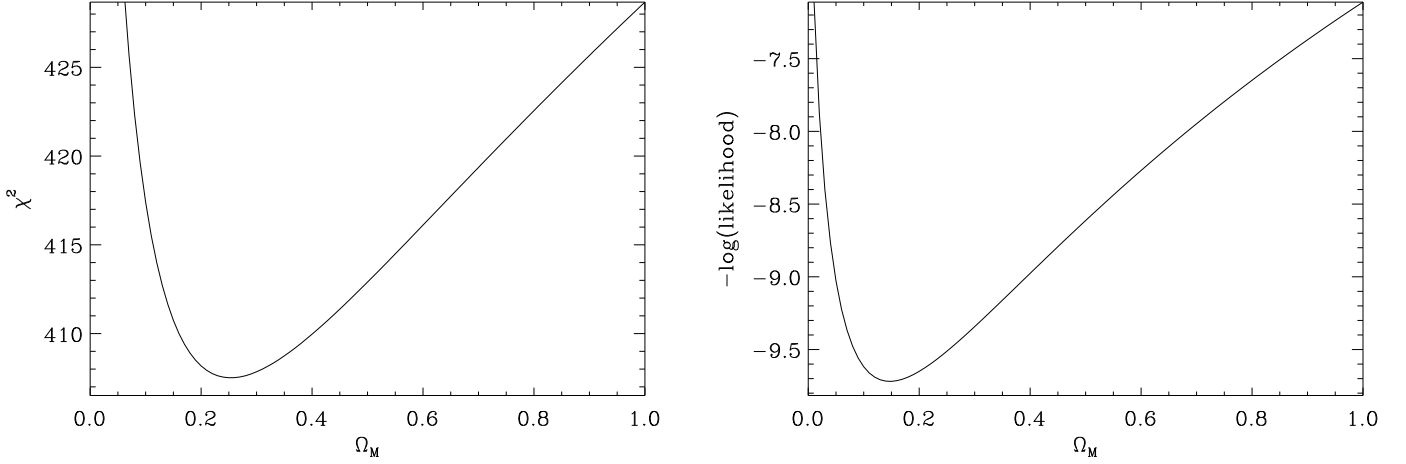


Figure 2. Value of the χ^2 of the simple power-law fit (left) and of the $-\log(\text{likelihood})$ of the fit with the MLM method which accounts for extrinsic variance (right) as a function of Ω_M in the assumption of a flat universe.

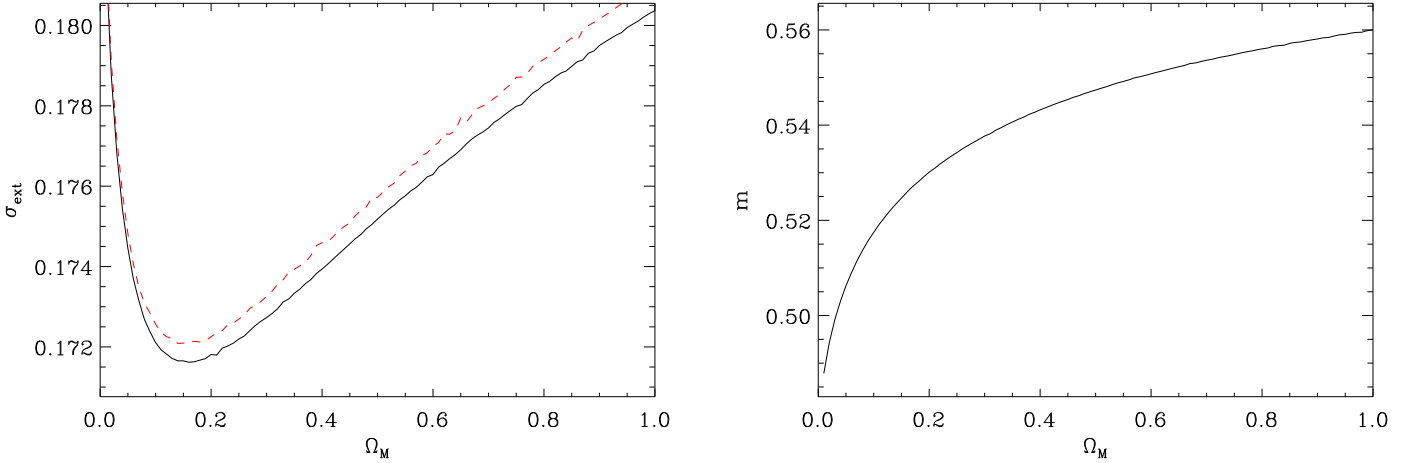


Figure 3. Value of the extrinsic scatter σ_{ext} (left) and power-law index m (right) as a function of Ω_M , obtained by fitting the correlation with the MLM method which accounts for extrinsic variance, for a flat universe. In the left panel, we also show, as a dashed line, the result obtained by using a different $\log(\text{likelihood})$ (see text).

$$\frac{1}{2} \sum_{i=1}^N \left[\log \left(\frac{1}{2\pi(\sigma_y^2 + m^2 \sigma_x^2 + \sigma_{y,i}^2 + m^2 \sigma_{x,i}^2)} \right) + \right. \\ \left. - \frac{(y_i - m x_i - q)^2}{\sigma_y^2 + m^2 \sigma_x^2 + \sigma_{y,i}^2 + m^2 \sigma_{x,i}^2} \right] \quad (1)$$

where, in our case, $\log(E_{p,i})$, $\sigma_x = 0$ and $\sigma_y = \sigma_{\text{ext}}$. We remark that setting $\sigma_x = 0$ does not affect the general validity of this formula.

As an example, the fit of the correlation with this method by using the E_{iso} values reported in Table 1 provides the following parameters value: $m = 0.54 \pm 0.03$, $K = 98 \pm 7$ and $\sigma_{\text{ext}} = 0.17 \pm 0.02$ (68% c.l.; consistent with the results reported by Amati 2006 for a smaller sample of 41 GRBs). In Figure 1 (right) we show the distribution of the normalised scatter of the data (see, e.g., Rossi et al. 2008 for details on the computation of this quantity) with superimposed the

normalised Gaussian. It is apparent that the scatter of the $E_{p,i} - E_{iso}$ correlation is indeed dominated by the extrinsic (i.e. non-Poissonian) variance.

For the goals of this paper, we repeated the above analysis by varying Ω_M , always under the assumption of a flat universe. Figure 2 (right) and Figure 3 (left) show that the values of the $-\log(\text{likelihood})$ and of the extrinsic variance σ_{ext} are indeed sensitive to Ω_M , both showing a clear minimum around $\Omega_M \sim 0.15$. Also the slope of the correlation is sensitive to the adopted cosmology, as shown in Figure 3 (right). By using the probability density function, the MLM also allows us to constrain Ω_M , that results to be in the range 0.04–0.40 at 68% and in the range 0.02–0.68 at 90% c.l (Table 2). An Ω_M value of 1 can be excluded at $\sim 99.9\%$ c.l.

If we release the flat universe hypothesis and let Ω_M and Ω_Λ vary independently (Figure 4, left), we still find ev-

Table 2. 68% and 90% c.l. ranges of Ω_M (both by assuming a flat universe or by letting Ω_M and Ω_Λ to vary independently) as determined with different methods applied to the present sample of 70 GRBs.

Method	c.l.	$\Omega_M(\text{flat})$	Ω_M	Ω_Λ
scatter	68%	0.04 – 0.40	0.04 – 0.50	<1.05
	90%	0.02 – 0.68	0.01 – 0.75	<1.15
scatter (self calib.)	68%	0.04 – 0.40	0.05 – 0.41	<1.05
	90%	0.02 – 0.67	0.01 – 0.73	<1.13
scatter ($m = 0.5$)	68%	0.03 – 0.28	0.03 – 0.33	<1.10
	90%	0.01 – 0.49	0.01 – 0.53	<1.17

idence for an universe with a low value of Ω_M (0.04–0.50 at 68% c.l.). Only an upper limit of ~ 1.05 can be set to Ω_Λ (see Table 2). This fact is not surprising, given that the redshift distribution of GRBs is expected to produce very vertically elongated contours in the $\Omega_M - \Omega_\Lambda$ plane (Ghirlanda et al. 2006; Kodama et al. 2008). The complementarity of GRB with other cosmological probes can be seen in Figure 4, where we plot, in addition to our results, the contours derived from SN Ia by Astier et al. (2006). As can be seen, already with the present sample of GRB, significantly improved constraints on Ω_M can be obtained by the combination of the two probes.

We have also investigated the estimate of the free parameters of the the inverse relation $X = mY + q$ plus the extrinsic scatter parameter $\sigma_{ext} = \sigma_x$. The results are fully consistent with previous ones and satisfy the expectation that $\sqrt{mm'} = r_{xy}$, where r_{xy} is the Pearson’s weighted linear-correlation coefficient (e.g., Bevington 1969, Bendat & Piersol 2000). For a flat universe with $\Omega_M = 0.3$, we find $m = 0.54$, $m' = 1.57$, $\sqrt{mm'} = 0.92$ and $r_{xy} = 0.92$.

Finally, we tested our results using the likelihood function suggested by Reichart (2001). The results obtained are fully consistent with the results above (Figure 2, left). This shows that the constraints that we have derived on the cosmological parameters do not depend significantly on the adopted statistical methodology and confirms the general soundness of our approach.

4 FUTURE PERSPECTIVES

4.1 Enrichment and redshift extension of the sample

In order to estimate the accuracy on cosmological parameters achievable by ongoing and future experiments, we have carried out a number of simulations based on an enriched sample of GRBs. By using the slope, normalization and extrinsic scatter of the $E_{p,i} - E_{iso}$ correlation obtained with the real sample of 70 GRBs and assuming, as an example, $\Omega_M = 0.27$, $\Omega_\Lambda = 0.73$, we generated 150 random GRBs with an accuracy on $E_{p,i}$ and E_{iso} of 20%. For 90% of the simulated GRBs, the redshift was randomly chosen from the GRB redshift distribution of our sample. For the remaining 10% of simulated GRBs we assumed a value of redshift larger than 6. The number of GRBs, and the accuracy on $E_{p,i}$ and E_{iso} , of the simulated sample are those that will realistically be provided in the next years by joint observations of *Swift* and GLAST/GBM (plus also Konus-Wind, Suzaku,

RHESSI, AGILE, etc.). Also the extension of the redshift distribution up to at least $z = 9$ is consistent both with theoretical predictions based on star formation rate evolution and the expected improvement in the sensitivity of hard X-ray and optical/near-infrared telescopes, that will be used to detect and follow-up GRBs and measure GRB redshift (e.g., Salvaterra et al. 2007 Salvaterra & Chincarini 2007).

In Figure 4 (right) we show the confidence level contours for Ω_M and Ω_Λ obtained by applying the method described in Section 3 to the sample made of the 70 “real” GRBs plus the 150 “simulated” ones. In Table 3, we report the constraints on cosmological parameters both in the assumption of a flat universe and by varying simultaneously Ω_M and Ω_Λ . A simple comparison with Table 2 shows that the simulated sample decreases the uncertainty range of Ω_M from 10 to only a factor 2. In addition, as can be seen in Figure 4 (right), significantly improved constraints on both Ω_M and Ω_Λ will be obtained by the combination of the contours obtained from GRBs with those from other probes, like, e.g., SN Ia.

Finally we note that the $E_{p,i} - E_\gamma$ correlation, because it needs the measure of a third observable (i.e. the break time in the optical afterglow light curve) requires the estimates of z and $E_{p,i}$ for a number of GRBs larger by more than a factor of 3 than required by the $E_{p,i} - E_{iso}$ correlation. For instance, the simulations performed by Ghirlanda et al. (2006) with 150 GRBs correspond to a “real” sample of at least ~ 500 GRBs having both z and $E_{p,i}$ measured.

4.2 Calibrating the $E_{p,i} - E_{iso}$ correlation

One of the main problems with the use of GRB correlations for cosmology is the lack of low-redshift GRBs (i.e. lying at $z < 1$) allowing for a cosmology-independent calibration similarly to type Ia SNe. This problem can be partly overcome by fitting the correlation in a sub-sample of GRBs lying at similar redshifts. This technique was proposed for future calibration of the slope of the $E_{p,i} - E_\gamma$ correlation (e.g., Ghirlanda et al. 2006), but can be effectively used for the $E_{p,i} - E_{iso}$ correlation, due to the much larger number of events that can be included in the $E_{p,i} - E_{iso}$ sample with respect to the $E_{p,i} - E_\gamma$ one. By studying the redshift distribution of the GRBs in our sample, we find that there are 18 events lying at redshift between ~ 0.8 and 1.2. The analysis of this sub-sample with the MLM method provides, indeed, evidence of a very low variation of m as a function of cosmological parameters. For instance, by assuming a flat universe, we find that the m best-fit values are in the range $m = 0.493 - 0.496$, to be compared to $m = 0.477 - 0.560$ obtained on the whole sample of 70 GRB. The value of m holds stable within this interval even by varying both Ω_M and Ω_Λ in the $[0,1]$ range. The dependence of m on the dark energy equation of state (parametrised as discussed in next section) is also within this interval. However, when taking into account the uncertainty resulting from the fits, the constraint on the calibrated slope of the $E_{p,i} - E_{iso}$ correlation becomes larger: $m = 0.44 - 0.55$, for both a flat and general universe. Thus, the applicability of the method is currently hampered by the large uncertainty affecting m , which results in a marginal improvements of the c.l. of cosmological parameters (Figure 5, left; Table 2). On the other hand, if we apply this calibration method to the simulated sample of

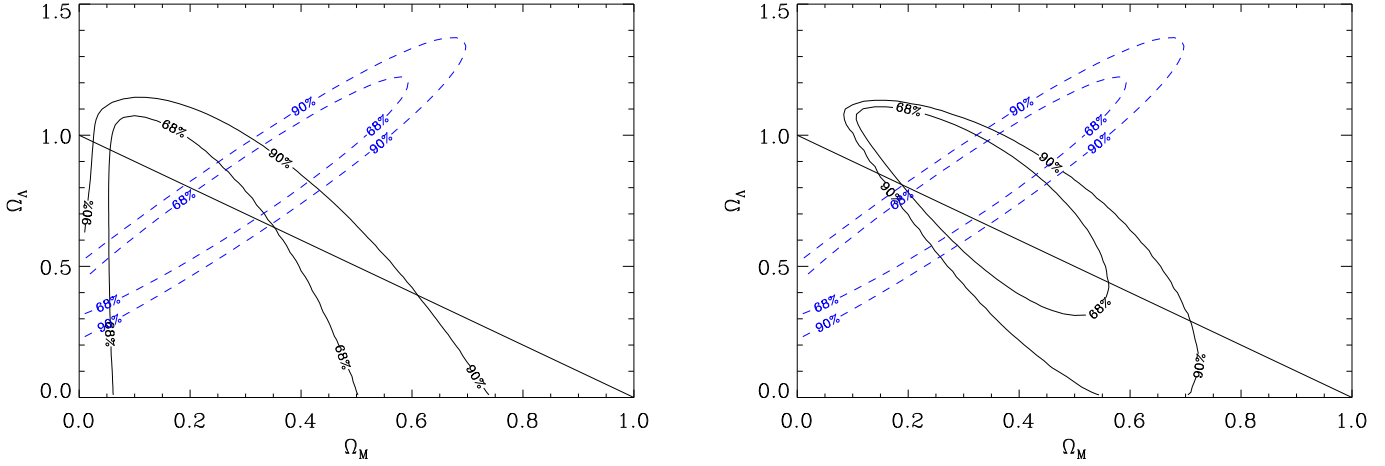


Figure 4. Contour confidence levels of Ω_M and Ω_Λ , obtained by fitting the correlation with the MLM method which accounts for extrinsic variance, with the present sample of 70 GRBs (left) and with the improved sample of 70 + 150 GRBs expected from next experiments (right; see text). In both panels we also show as blue dashed contours the constraints derived from SN Ia by Astier et al. (2006).

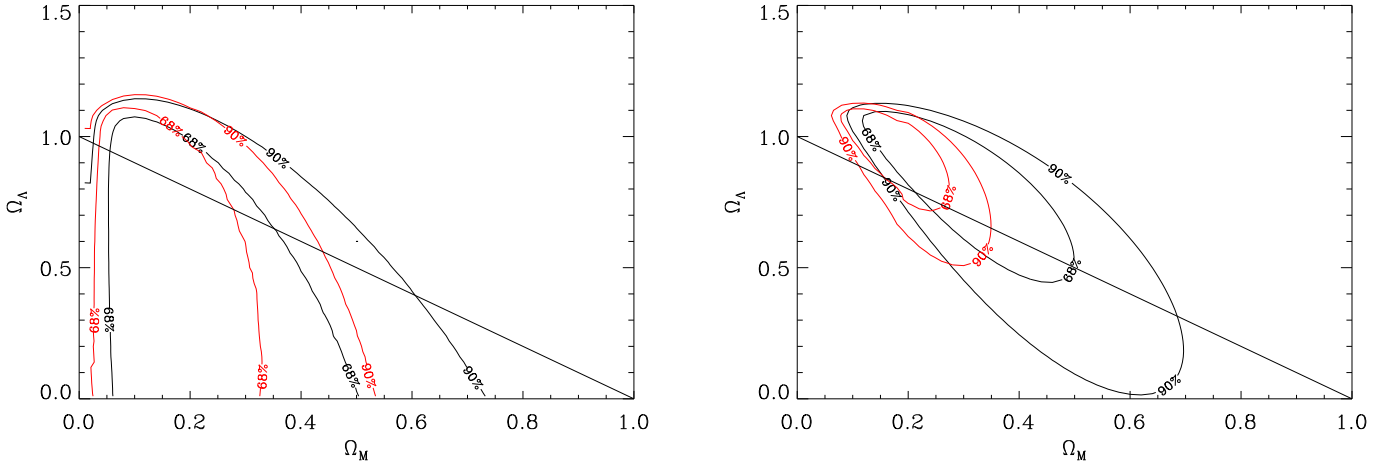


Figure 5. Contour confidence levels of Ω_M and Ω_Λ obtained by fitting the correlation with MLM method which accounts for extrinsic variance with m calibrated based on GRBs lying at $0.8 < z < 1.2$ (black contours) and m fixed at 0.5 (red contours); see text. Left: present sample of 70 GRB; right: improved sample of present 70 GRBs + 150 GRBs expected from next experiments.

70 + 150 GRB, the improvement in the estimates of cosmological parameters is significant (see Table 3 and compare Figure 5, right, with Figure 4, right).

A second possibility to calibrate the slope of the correlation is to derive it on robust physical basis. Several analyses reported above or elsewhere (e.g., Ghirlanda et al. 2008) point out a slope of $m=0.5$. This value is also predicted by several theoretical models, involving in various forms synchrotron, inverse Compton, thermal and Comptonised thermal emissions; see, e.g., Zhang & Mészáros (2002); Thompson et al. (2007). Figure 5 (red contours) and Table 3 illustrate quite clearly that the correlation fitted with the MLM method after assuming $m = 0.5$ improves significantly the accuracy degree of the cosmological parameter measurements.

4.3 Investigating the evolution of the dark energy

The GRB redshift distribution extends up to $z > \sim 6$, which is well above that of SNe-Ia ($z \sim 1.7$). Therefore, at least in principle, GRBs are powerful tools to study the evolution of dark energy with the redshift. In the following, we adopt the parametrization of the dark energy equation of state proposed by Chevallier & Polarski (2001); Linder & Utherer (2005), i.e. $P = w(z)\rho$, where:

$$w(z) = w_0 + \frac{w_a z}{1 + z} \quad (2)$$

As shown in Figure 6 (left), with our sample of 70 GRBs we find that the $-\log(\text{likelihood})$ computed with the MLM by assuming a flat universe with $\Omega_M = 0.27$ and by setting $w_a = 0$ is indeed sensitive to w_0 , with a minimum

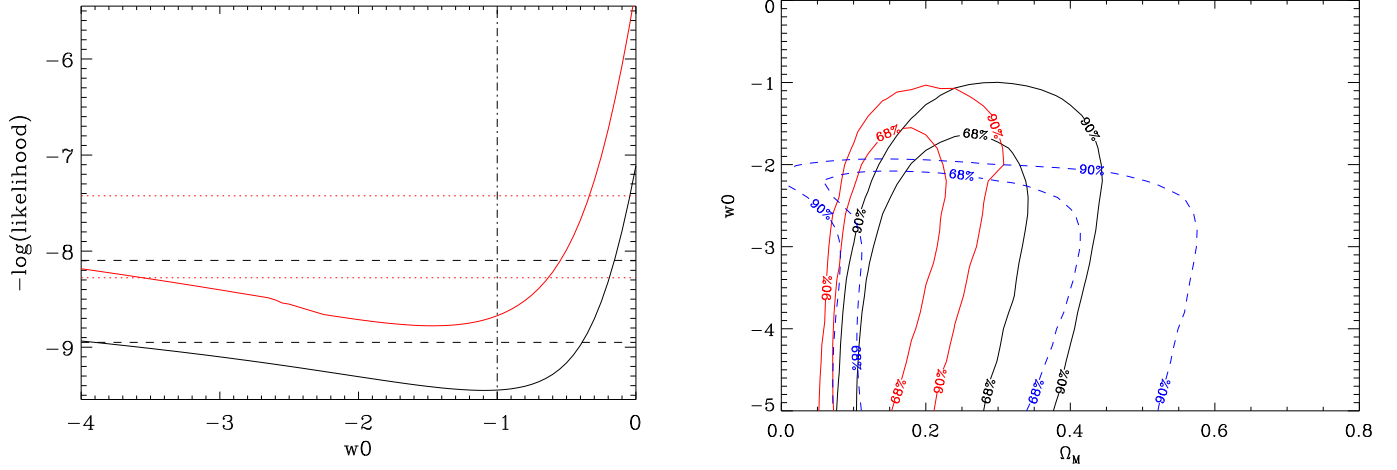


Figure 6. Left: Value of the $-\log(\text{likelihood})$ as a function of the parameter of the dark energy equation of state w_0 (see text) in the assumption of a flat universe with $\Omega_M = 0.27$ and $\Omega_\Lambda = 0.73$ obtained with the present sample of 70 GRB. Right: contour confidence levels of Ω_M and w_0 in the assumption of a flat universe obtained with the improved sample of present 70 GRBs + 150 GRBs expected from next experiments (continuous line: $w_a = 0$; dashed lines: $w_a = 4$). In both figures, the red lines indicate the results obtained by fixing m at 0.5.

Table 3. 68% and 90% c.l. ranges of Ω_M (both by assuming a flat universe or by letting Ω_M and Ω_Λ to vary independently) as determined with different methods applied to a sample composed by the present sample of 70 GRBs plus 150 simulated GRBs with known z and $E_{p,i}$ expected to be provided in the near future by present and planned GRB experiments (see text).

Method	c.l.	$\Omega_M(\text{flat})$	Ω_M	Ω_Λ
scatter	68%	0.21 – 0.50	0.11 – 0.57	0.35 – 1.12
	90%	0.16 – 0.66	0.08 – 0.73	<1.15
scatter (self calib.)	68%	0.22 – 0.48	0.12 – 0.49	0.47 – 1.10
	90%	0.17 – 0.59	0.10 – 0.69	0.10 – 1.11
scatter ($m = 0.5$)	68%	0.13 – 0.27	0.18 – 0.28	0.62 – 1.10
	90%	0.11 – 0.35	0.06 – 0.35	0.50 – 1.12

around -1 (corresponding to a cosmological constant). Unfortunately, within the limits of present GRB sample no significant constraints on w_0 can be provided. Even after assuming $m = 0.5$, w_0 can be constrained only to be between -3.7 and -0.7 at 68% c.l. In Figure 6 (right) we show the $\Omega_M - w_0$ confidence level contours obtained with the sample of 70 real + 150 simulated GRBs by assuming a flat universe with $w_a = 0$ (continuous lines) and $w_a = 4$ (dashed line). As can be seen, such a sample would provide clear evidence of $w_0 < -1$ and some hints on w_a .

5 CONCLUSIONS

We have used an updated sample of 70 GRBs aimed at deriving the cosmological parameters Ω_M and Ω_Λ from the $E_{p,i} - E_{\text{iso}}$ correlation of GRBs. With respect to previous attempts mainly based on the $E_{p,i} - E_\gamma$ and $E_{p,i} - E_{\text{iso}} - T_{0.45}$ correlations, the use of $E_{p,i} - E_{\text{iso}}$ correlation has the advantages of requiring only two parameters, both directly inferred from observations. This fact allows for the use of a richer sample of GRBs (e.g., a factor 3-4 larger than used in the $E_{p,i} -$

E_γ correlation), and a reduction of systematics, with respect to three-parameters spectrum-energy correlations.

Our method consists of studying the dependence of the dispersion of the $E_{p,i} - E_{\text{iso}}$ correlation on cosmological parameters by adopting a maximum likelihood method, which allowed us to parameterise and quantify correctly the extrinsic (i.e. non-Poissonian) scatter component. From our analysis, a number of significant results do emerge:

a) a simple power-law fit shows a clear trend of the dispersion, with a minimum at $\Omega_M = 0.2-0.4$ (for a flat universe). By refining the fit with the MLM, we found that both the extrinsic variance and the slope of the correlation show a significant dependence on cosmology. From the study of the $\log(\text{likelihood})$ we derived $\Omega_M = 0.04-0.40$ at 68% c.l. and $0.02-0.68\%$ at 90% confidence levels;

b) after assuming “a priori” a slope $m = 0.5$, consistently with both observations and the predictions of several models for GRB prompt emissions, we derive $\Omega_M = 0.01-0.49$ at 90%;

c) if we release the assumption of a flat universe, we still find evidence for a value of $\Omega_M < 1$ ($0.04-0.50$ at 68% c.l.) and a weak dependence of the dispersion of the $E_{p,i} - E_{\text{iso}}$ correlation on Ω_Λ with an upper limit of 1.15 (90% c.l.);

d) our study does not make assumptions on the $E_{p,i} - E_{\text{iso}}$ correlation or make use of independent calibrators to set the “zero point” of the relation, therefore our approach does not suffer from circularity and provides independent evidence for the existence of a gravitationally repulsive energy component (“dark energy”) which accounts for a large fraction of the energy density of the universe;

e) in a flat universe, the $E_{p,i} - E_{\text{iso}}$ correlation is also (weakly) sensitive to the w_0 parameter of the equation of state of dark energy;

f) we have simulated the impact of ongoing/planned GRB experiments (e.g., *Swift* + GLAST) on the future Ω_M and Ω_Λ measurements and shown that the uncertainties can

be decreased by almost an order of magnitude with respect to those obtained with the current GRB sample.

REFERENCES

- Amati L. et al., 2002, *A&A*, 390, 81
 Amati L., 2006, *MNRAS*, 372, 233
 Amati L. et al., 2007, *A&A*, 463, 913
 Astier P. et al. 2006, *A&A*, 447, 31
 Bendat J.S., Piersol A.G., 2000, "Random Data: Analysis and Measurement Procedure – 3rd ed.", Wiley Series in Probability and Statistics, John Wiley & Sons, Inc., New York (USA)
 Bevington P.R., 1969, "Data Reduction and Error Analysis for the Physical Sciences", McGraw-Hill, New York (USA)
 Butler N.R., Kocevski D., Bloom J.S., Curtis J.L., 2007, *ApJ*, 671, 656
 Cabrera I.J. et al., 2007, *MNRAS*, 382, 342
 Campana S. et al., 2006, *Nature*, 442, 1008
 Campana S. et al., 2007, *A&A*, 472, 395
 Cenko S.B., Kasliwal M., Harrison F.A., 2006, *ApJ*, 652, 490
 Chevallier M., Polarski D., 2001, *Int. J. Mod. Phys.*, D10, 213
 D'Agostini G., 2005, physics/0511182
 De Bernardis P. et al., 2003, *Nature*, 404, 955
 Dunkley J. et al., 2008, *ApJS*, submitted (arXiv:0803.0586)
 Eisenstein D.J. et al., 2005, *ApJ*, 633, 560
 Firmani C. et al., 2006, *MNRAS*, 370, 185
 Ghirlanda G., Ghisellini G., Lazzati D., 2004, *ApJ*, 616, 331
 Ghirlanda G., Ghisellini G., Firmani C., 2006, *New Journal of Physics*, 8, 123
 Ghirlanda G., Nava L., Ghisellini G., Firmani C., 2007, *A&A*, 466, 127
 Ghirlanda G., Nava L., Ghisellini G., Firmani C., Cabrera J.L., 2008, *MNRAS*, 387, 319
 Golenetskii S. et al., 2006, *GCN* 4539
 Golenetskii S. et al., 2006, *GCN* 4989
 Golenetskii S. et al., 2006, *GCN* 5460
 Golenetskii S. et al., 2007, *GCN* 6049
 Golenetskii S. et al., 2007, *GCN* 6879
 Golenetskii S. et al., 2007, *GCN* 6960
 Golenetskii S. et al., 2007, *GCN* 7114
 Golenetskii S. et al., 2008, *GCN* 7482
 Golenetskii S. et al., 2008, *GCN* 7487
 Golenetskii S. et al., 2008, *GCN* 7589
 Guidorzi C. et al., 2006, *MNRAS*, 371, 843
 Kodama Y. et al., 2008, *MNRAS*, in press (arXiv:0802.3428)
 Komatsu J. et al., 2008, *ApJS*, submitted (arXiv:0803.0547)
 Krimm H., et al., 2006, *AIP Proc.*, 836, 145
 Landi R., Amati L., Guidorzi C., Frontera F., Montanari E., 2006, *Nuovo Cimento B*, 121, 1503
 Liang N., Xiao W.K., Liu Y., Zhang S.N., 2008, *ApJL*, 685, 354
 Linder E.V., Utherer D., 2005, *PhRvD*, 72, 3509
 Mészáros P., 2006, *Prog.Phys*, 69, 2269
 Mundell C.G. et al. 2007, *ApJ*, 660, 489
 Percival W.J. et al. 2007, *MNRAS*, 381, 1053
 Perley C.G. et al. 2008, *ApJ*, 672, 449
 Perlmutter S. et al. 1998, *Nature*, 391, 51
 Perlmutter S. et al. 1999, *ApJ*, 517, 565
 Reichart D.E., 2001, *ApJ*, 553, 235
 Riess A.G. et al., 1998, *ApJ*, 116, 1009
 Riess A.G. et al., 2004, *ApJ*, 607, 665
 Rosati P., Borgani S., Norman C., 2002, *ARA&A*, 40, 539
 Rossi et al., 2008, *MNRAS*, 388, 1284
 Sakamoto T. et al., 2005, *ApJ*, 629, 311
 Sakamoto T. et al., 2008, *ApJS*, 175, 169
 Sakamoto T. et al., 2008, *ApJ*, 679, 570
 Salvaterra R., Campana S., Chincarini G., Covino S., Tagliaferri G., 2007, *MNRAS*, 385, 189
 Schaefer B.E., 2007, *ApJ*, 660, 16
 Spergel D.N. et al., 2003, *ApJS*, 148, 175
 Stratta G. et al., 2006, *A&A*, 461, 485
 Tagliaferri G. et al., 2005, *A&A*, 443, L1
 Tegmark M. et al., 2006, *PhRvD*, 74, 3507
 Thompson T. et al., 2007, *ApJ*, 602, 875
 Ulanov M.V. et al., 2005, *Nuovo Cimento C*, 28, 351
 Voit G.M. et al., 2005, *Rev.Mod.Phys*, 77, 207
 Zhang, B., Mészáros, P., 2002, *ApJ*, 581, 1236